

THE RELAXATION PHENOMENON IN PROPER UNIAXIAL FERROELECTRIC–SEMICONDUCTOR CRYSTALS $\text{Sn}_2\text{P}_2\text{S}(\text{Se})_6$ WITH INCOMMENSURATE PHASE

Yu. Vysochanskii, A. Molnar

*Institute of Solid State Physics and Chemistry, Uzhgorod University
46 Pidhirna Str., UA-294000, Uzhgorod, Ukraine*

(Received August 27, 1996)

For ferroelectric–semiconductor crystals $\text{Sn}_2\text{P}_2\text{S}(\text{Se})_6$ the relaxation of electron subsystem determines the Lifshitz point shift on the phase diagram and the pinning of order parameter wave (memory effect) in the incommensurate phase. For these proper uniaxial ferroelectrics both effects are agreeably described by the phenomenological model, which assumes: the renormalization of the spatial dispersion of the stiffness coefficient for the order parameter fluctuations due to the relaxational variation of the charge carriers concentration on the impurity energy level in the forbidden band of the crystal; the local centres energy modulation, caused by the non-uniform static field of the order parameter in the IC-phase leading to the appearance of concentration-wave of the charge carriers.

Key words: Ferroelectric–semiconductor crystals, Lifshitz point, phase diagram, order parameter.

PACS number(s): 77.80 Rh, 77.80.Bh

I. INTRODUCTION

One of the most interesting non-equilibrium phenomena, which characterises incommensurate (IC) systems, is the memory effect. If crystal is kept in the IC phase at a certain stable temperature T_{st} for a sufficiently long time, then, on passing this temperature again, anomalies of various physical properties are observed. This is caused by the formation of a phase with fixed wave vector within the IC phase, which becomes locked in a certain temperature region around T_{st} due to the pinning of the IC modulation. The memory effect has been observed in various IC systems including proper and improper ferroelectrics [1]. In all cases the effect has been attributed to the coupling of mobile defects to the modulation order parameter [2], forcing the defects to diffuse in the IC modulated potential. However, the nature of the defects and their interaction with local order parameter remain unknown. Mobile charged defects also play a special role in the critical behaviour of crystals. For instance, in ferroelectric semiconductors the instability of the crystalline structure is related to the kinetics of the electronic subsystem. The variation of the electron concentration on the attachment levels can change the Lifshitz point (LP) and tricritical point (TCP) positions on the phase diagram and considerably modify the critical anomalies of the crystal's thermodynamic characteristics [3]. One can expect effects of prolonged relaxation of crystal properties to manifest themselves in both the IC phase (anomalous temperature hysteresis, the memory effect) and the vicinity of the transition directly from the initial high-symmetry phase to the commensurate low-symmetry phase. The aim of this work is to study the relaxation phenomenon in ferroelectric–semiconductor $\text{Sn}_2\text{P}_2\text{S}_6$ and $\text{Sn}_2\text{P}_2\text{Se}_6$. On the phase diagram of the $\text{Sn}_2\text{P}_2(\text{Se}_x\text{S}_{1-x})_6$ solid solution at $x_{LP} \approx 0.28$ the Lifshitz point exists [4]. $\text{Sn}_2\text{P}_2\text{S}_6$ crystal is proper fer-

roelectric and undergoes second order phase transition (PT) from the paraelectric ($\text{P}2_1/c$) to the ferroelectric ($\text{P}c$) phase at $T_0 \approx 337$ K. For the $\text{Sn}_2\text{P}_2\text{Se}_6$ crystal the intermediate IC phase exists between $T_i \approx 221$ K and $T_c \approx 193$ K. The dielectric [5] and optic [6] methods were used for non-equilibrium processes studying.

Part 2 compares the data on the investigations of the memory effect in the IC-phase for the $\text{Sn}_2\text{P}_2\text{Se}_6$ crystals by measuring the temperature dependence of the birefringence and the low-temperature dielectric constant for the samples with different resistivity and depending on the illumination effect. The results of studies of the long-term relaxation effect of the dielectric parameters in the paraelectric phase and the appearance of an intermediate state between the paraelectric and ferroelectric phases for the $\text{Sn}_2\text{P}_2\text{S}_6$ crystals are given in Part 3. The phenomenological analysis and a comparison between the relaxation effects in the IC- and paraelectric phases for the ferroelectrics–semiconductors studied are presented in Part 4.

II. THE MEMORY EFFECT AND RELAXATIONS IN INCOMMENSURATE PHASE IN $\text{Sn}_2\text{P}_2\text{Se}_6$ CRYSTALS

The non-equilibrium of the IC phase in the $\text{Sn}_2\text{P}_2\text{Se}_6$ crystals was studied by measuring the temperature dependence of optical birefringence $\Delta n(T)$. The Senarmont method was used for the study of vapour–transport grown $\text{Sn}_2\text{P}_2\text{Se}_6$ crystals [6].

The results of birefringence studies of the $\text{Sn}_2\text{P}_2\text{Se}_6$ crystals in case of the light beam oriented along [001] crystallographic direction are presented in fig. 1. The $\Delta n(T)$ dependence has a break at $T_i \approx 221$ K, while at $T_c \approx 193$ K a leap is observed. The behaviour of that type corresponds to the second order PT at T_i and first

order PT at T_c . The studies were carried out in a cooling mode with pre-annealing for 2 hours at 370 K to eliminate the influence of inner fields.

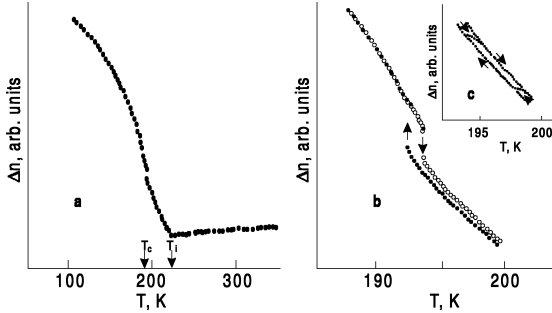


Fig. 1. Temperature dependence of the $\text{Sn}_2\text{P}_2\text{Se}_6$ crystal birefringence (a), hysteresis in the vicinity of T_c (b) and anomalous hysteresis loops in the incommensurate phase (c) [6].

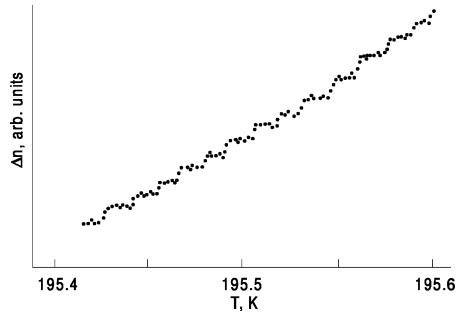


Fig. 2. Temperature dependence of birefringence of $\text{Sn}_2\text{P}_2\text{Se}_6$ incommensurate phase at the temperature change rate 0.4 K/hours [6].

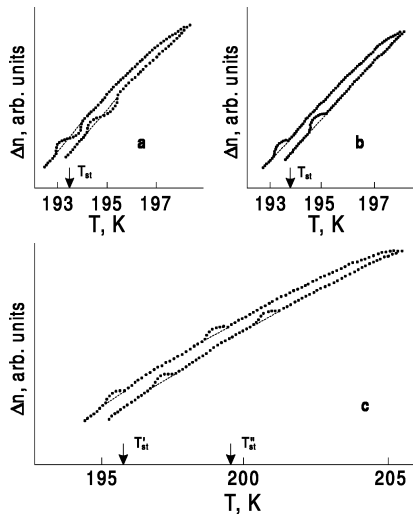


Fig. 3. The memory effect in birefringence of $\text{Sn}_2\text{P}_2\text{Se}_6$ incommensurate phase at various times of temperature stabilization: a — 8h, b — 3h, c — consecutive three-hour stabilization at temperatures T'_{st} and T''_{st} [6].

The $\Delta n(T)$ data obtained in cooling and heating modes are compared in fig. 1, b. The temperature hysteresis for PT from the IC-phase to the ferroelectric phase is observed ($\Delta T_c \approx 1$ K). The amplitude of the hysteresis decreases smoothly within the IC-phase and vanishes at T_i . The hysteresis value depends on the spontaneous birefringence value, $\Delta T_h(\Delta n_s)$ almost linearly [6]. This confirms the fact that the value of hysteresis is proportional to the mean-square value of the order parameter. When the temperature within the IC-phase is cycled, specific loops are observed (see fig. 1, c) similar to those found in the dielectric studies (fig. 5). No relation between hysteresis and temperature variation rate has been found. This rate was varied from 3 K per hour to 0.4 K per hour. However, when the rate reached 0.4 K per hour, a crossover from the continuous behaviour of $\Delta n(T)$ to the stepwise behaviour was observed (fig. 2).

In [6] we have also studied in detail the thermal memory effect in $\text{Sn}_2\text{P}_2\text{Se}_6$. Being annealed at $T = 370$ K, the crystal was then cooled and kept in the IC-phase at T_{st} for 3 hours. Temperature stabilization was not worse than 0.02 K. After cooling to the ferroelectric phase, the specimen was heated at low rate. It is seen (fig. 3, b) that at $T_{st} + \Delta T_h$ a slight deviation of $\Delta n(T)$ from smooth dependence occurs on the heating curve. Here ΔT_h is an anomalous hysteresis value. In the cooling mode, the deviation occurs at T_{st} . This deviation remains even after the crystal was kept in the ferroelectric phase for 15 hours and after a brief exposure in the paraelectric phase. It vanishes, however, after annealing with light off at $T_i + 1$ K for 1 hour. These results were obtained with the laser on during the temperature stabilization. In order to reach the same situation when the laser is off, one should stabilize the temperature at T_{st} for 8 hours. At the same time, stabilization for 8 hours with the laser on results in the variation of anomalous deviation of $\Delta n(T)$, i.e. a bend point appears (fig. 3). In case of heating, this point is shifted upwards by the hysteresis value, while in case of cooling, its position coincides with the stabilization temperature. Similarly to a 3-hour experiment, the deviation remains after a protracted exposure in the ferroelectric phase (for 15 hours) and vanishes during the specimen exposure in the paraelectric phase (for 1 hour). In case of a brief exposure of specimen in the paraelectric phase, the record is not cleared. Note that illumination upon stabilization promotes memory effect appearance, while that in the ferroelectric phase reduces its amplitude. Fig. 3, c illustrates the result of sequential stabilization for 3 hours at two temperature values with the laser on. It is seen that two memory effect anomalies are clearly observed upon heating and cooling. Note that the memory effect record does not affect both the behaviour of the $\Delta n(T)$ dependence in the vicinity of the PT from the IC-phase to the ferroelectric phase and the value of T_i [6].

The dielectric measurements were made at the frequency of 10 kHz [5]. The system of thermostating and measuring the dielectric response of the sample was computer controlled. The measuring field was 0.05 V/cm. The relative error in measuring ϵ' was 0.1% and that in

measuring ε'' was 0.5%. The temperature was stabilized to within ± 0.002 K, and the rate of temperature change was varied within 0.3–0.01 K/min. The experiments have been carried out on [100] oriented samples with the typical size of $2 \times 2 \times 1$ mm³ cut from the Sn₂P₂Se₆ crystals grown using vapour transport and Bridgeman techniques. Gold electrodes were evaporated on the (100) faces. The Sn₂P₂Se₆ crystals grown by these two methods differ essentially in electroconductivity. In particular, the Bridgeman-type sample used in the experiment had a specific conductivity at the room temperature of about 10^{-10} Ω⁻¹.cm⁻¹, while the conductivity of the vapour-transport type sample was about 10^{-7} Ω⁻¹.cm⁻¹.

It should be noted that these two kinds of crystals differ noticeably also in other properties. For instance, the crystals of the Bridgeman type exhibit a very large domain wall contribution to the dielectric constant below the lock-in phase transition, typical of proper ferroelectrics with an incommensurate phase. The domain wall contribution in vapour-transport-type crystals is much smaller.

In fig. 4 the temperature dependence of the dielectric constant for the Bridgeman-type (B) and the vapour-transport-type (V) Sn₂P₂Se₆ crystals are shown at the cooling mode in a wide temperature region. We can see the Curie-Weiss-type $\varepsilon'(T)$ dependence in the paraelectric phase of sample B. In the case of V-sample electroconductivity has a very strong influence on $\varepsilon'(T)$ behaviour. Some difference also appears for $\varepsilon'(T)$ in the incommensurate phase of these two samples. In the ferroelectric phase for B crystal we observe a very strong dielectric response from the domain wall. For B crystal the memory effect does not appear at temperature stabilization in darkness till 12 hours (fig. 5). At the same time temperature stabilization at white light illumination gives us the memory effect appearance with small amplitude (fig. 5). In this case after memory recording the stepwise $\varepsilon'(T)$ behaviour appear at $T < T_{st}$ like the birefringence temperature dependence at small rate of temperature changes (fig. 2).

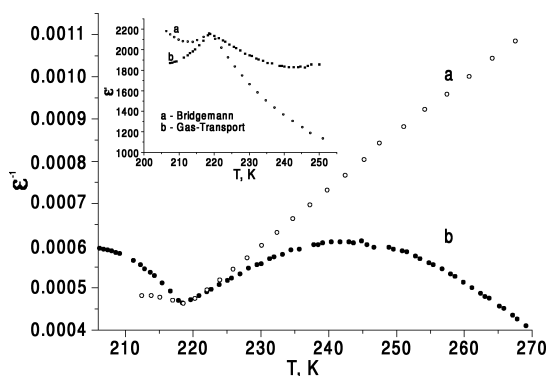


Fig. 4. Temperature dependence of dielectric constant in the vicinity of paraelectric-incommensurate phase transition for the Bridgeman type (a) and the vapour transport type (b) Sn₂P₂Se₆ crystals.

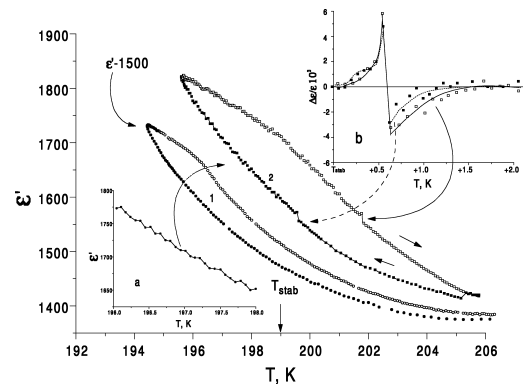


Fig. 5. Results of the memory effect recording in the IC phases of the Bridgeman type Sn₂P₂Se₆ crystal at stabilization time 12 h and temperature $T_{st} = 199$ K in darkness (4.1) and at white light illumination (4.2). On inserts: the step-like $\varepsilon'(T)$ behaviour at $T < T_{st}$ after memory effect recording (a); the reduced anomalous part of dielectric constant which related to memory effect (b).

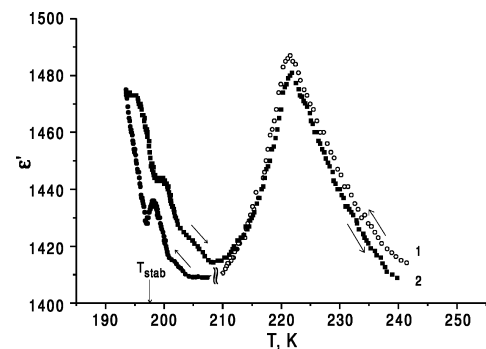


Fig. 6. Shape of dielectric constant temperature dependence anomaly at phase transition from the paraelectric to the IC phase ($T_i = 221$ K) before (4.1) and after (4.2) the memory effect recording at 2 hours and $T_{st} = 197.5$ K for the vapour transport type Sn₂P₂Se₆ crystal.

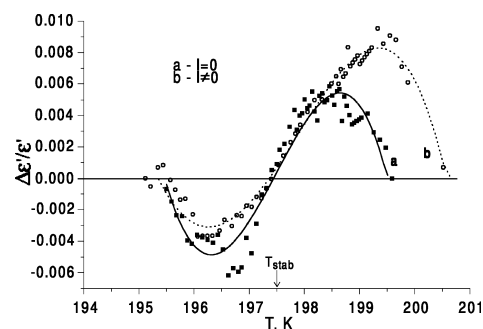


Fig. 7. Memory effect in the vapour-transport type Sn₂P₂Se₆ crystals on cooling $\varepsilon(T)$ curve recorded at stabilization time 2 h and temperature $T_{st} = 197.5$ K in darkness (a) and under white light illumination at temperature stabilization (b). The solid and dashed lines are demonstrating the results of the polynomial extrapolation.

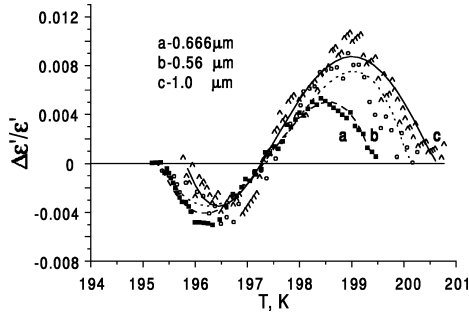


Fig. 8. Memory effect for the condition on Figure 6 at different wavelengths of light.

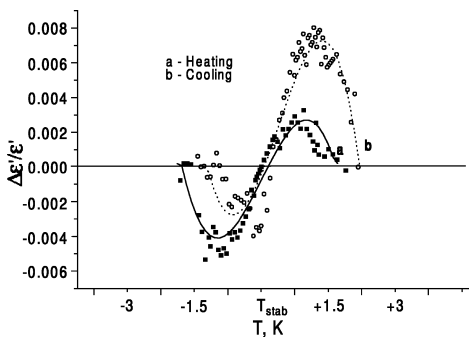


Fig. 9. Temperature dependence of the reduced anomalous part of the dielectric constant associated with the memory effect (from Figure 6) at heating and cooling regimes.

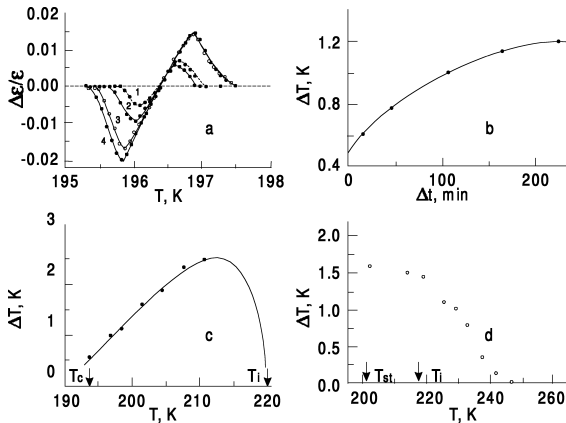


Fig. 10. a — temperature dependence of the dielectric constant reduced anomalous part associated with the memory effect at varying stabilization times ($T_{st} = 196.4$ K): 1 — 15 min, 2 — 45 min, 3 — 120 min, 4 — 230 min; b — dependence of the temperature interval ΔT between the maximum and minimum of the $\Delta\varepsilon/\varepsilon$ on the stabilization time ($T_{st} = 196.5$ K). The solid line — the result of fitting by exponential law [7]; c — dependence of the temperature interval ΔT between the maximum and minimum of $\Delta\varepsilon/\varepsilon$ on the stabilization temperature. The stabilization time was 120 min. The solid line is a fit obtained with equation (4.11); d — the variation of the width of the locked phase on heating the sample above the stabilization temperature.

The memory effect is very distinctly pronounced for a V-type crystal already after a 2 hours exposure in darkness (fig. 6). We must point out that after “memory” recording we do not see any change in the $\varepsilon'(T)$ anomaly at the vicinity of PT from the paraelectric to the incommensurate phase (fig. 6). The amplitude and temperature interval of memory effect both increase if we illuminate the sample with a white light at the process of temperature stabilization (fig. 7). It is important that the spectral sensitivity of memory recording has been observed (fig. 8). This effect is the strongest at crystal being illuminated by the monochromatic light with $\lambda=1 \mu\text{m}$. It is important that the shape of the memory effect anomalies in $\varepsilon'(T)$ is nonsymmetric (fig. 7). The asymmetry we have observed for birefringence (fig. 3, b). The asymmetry changes were observed after the transition from the cooling of the sample to its heating (fig. 9). After two successive temperature stabilizations two anomalies appear. The location of the anomalies on the cooling and heating curves are shifted in temperature by the magnitude of the global temperature hysteresis. The cooling of the sample down into the ferroelectric phase leaves the induced anomalies unaltered. So, the peculiarities of the memory effect in dielectric susceptibility coincide with those in birefringence data (fig. 3).

In fig. 10 the temperature dependence of the relative anomalous parts of the dielectric susceptibility associated with the memory effect are presented for several stabilization times. It is obvious that the amplitude and the width of the anomaly grow with an increase in stabilization time. Further, upon an increase in the stabilization temperature, the temperature interval ΔT between the minimum and maximum of $\Delta\varepsilon/\varepsilon(T)$ shows an increase. It should be mentioned that, because of high dielectric losses at $T \geq 212$ K, it was impossible to trace this temperature variation up to the IC phase transition (T_i) [7].

Heating the sample within the IC phase up to T_i leaves the memory effect anomaly almost unaltered. However an increase in temperature above T_i is accompanied by a gradual suppression of the memory effect anomaly. Finally, heating the crystal above approximately 245 K results in a complete disappearance of the memory effect (fig. 10).

III. THE RELAXATIONAL APPEARANCE OF INCOMMENSURATE PHASE IN $\text{Sn}_2\text{P}_2\text{S}_6$ CRYSTALS

Now we shall analyse the experimental data on the long time relaxation process in the paraelectric phase for the $\text{Sn}_2\text{P}_2\text{S}_6$ compound which has the second order ferroelectric phase transition directly from para- to ferroelectric phase. Our investigations were carried out with a $6 \times 6 \times 3 \text{ mm}^3$ samples fabricated from a $\text{Sn}_2\text{P}_2\text{S}_6$ single crystals grown by the Bridgeman and vapour-transport methods. The electric contacts were formed by the thermal deposition of gold on the (100) polar cuts. Here we shall discuss the experimental data for the Bridgeman

type crystals.

The temperature dependence of ϵ' for the $\text{Sn}_2\text{P}_2\text{S}_6$ was measured during cooling after annealing for three hours in the paraelectric phase at 373 K. At a cooling rate of 0.1 K/min the ϵ' vs T dependence obeys the Curie-Weiss law within a broad temperature range (for the vapour type $\text{Sn}_2\text{P}_2\text{S}_6$ crystal we have observed clearly the logarithmic deviation from Curie-Weiss law in the paraelectric phase at $T \leq T_0 + 10$ K (fig. 11) [8]). The ϵ^{-1} vs T dependence is extrapolated to a zero value at $T_0 \approx 335.2$ K, while the temperature corresponding to the maximum in the ϵ' vs. T dependence is 335.95 K. When the cooling rate of the sample was reduced, a departure from the above-mentioned law was observed. The value of ϵ' decreased in the temperature interval from T_0 to $T_0 + 2$ K. The temperature of the maximum in the ϵ' vs. T dependence lowers in the process.

Prolonged temperature stabilization in the paraelectric phase at $T > T_0 + 2$ K does not (to within 1%) cause a change in ϵ' . However, the temporal relaxation of ϵ' was noticeable in the T_0 to $T_0 + 2$ K range and also in the ferroelectric phase. The temporal variation of the dielectric constant is described by the exponential law

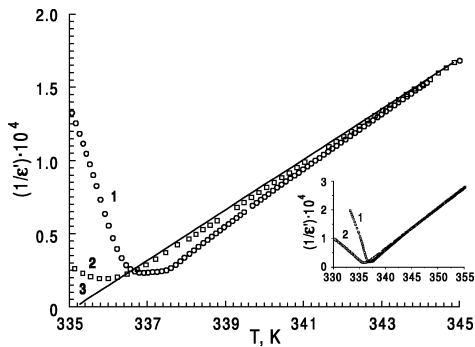


Fig. 11. Temperature dependence of dielectric constant inverse value for vapour transport grown (4.1) and Bridgeman method grown (4.2) $\text{Sn}_2\text{P}_2\text{S}_6$ crystals. The solid line (4.3) obeys the Curie-Weiss law.

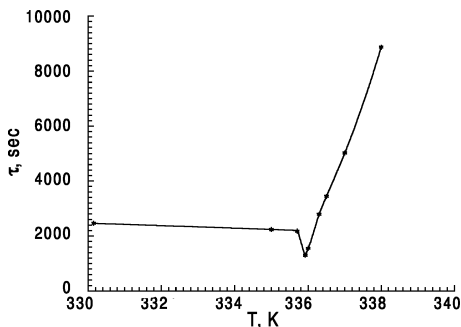


Fig. 12. The temperature dependence of relaxation time τ for $\text{Sn}_2\text{P}_2\text{S}_6$ crystal in the vicinity of ferroelectric phase transition.

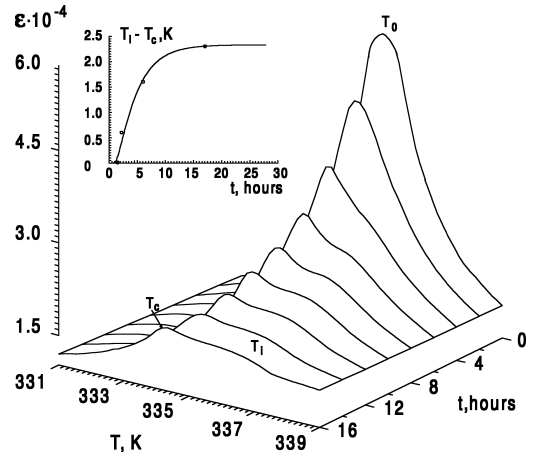


Fig. 13. The temperature dependence of the dielectric constant of the $\text{Sn}_2\text{P}_2\text{S}_6$ crystal after exposure at $T=336.2$ K. The insert depicts the temporal dependence of the temperature interval $T_1 - T_c$ at the same exposure temperature (the points stand for the experimental data, and the curve represents the calculated results by relation (4.5)) [5].

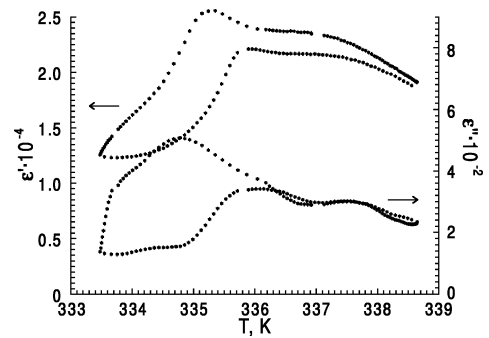


Fig. 14. The temperature hysteresis of $\epsilon'(T)$ and $\epsilon''(T)$ after the $\text{Sn}_2\text{P}_2\text{S}_6$ sample stabilization at temperature $T = 336.2$ K for six hours.

$$\epsilon|_t = \epsilon|_0 + \Delta\epsilon|e^{-\frac{t}{\tau}}$$

We established that there is a difference between the relaxation mechanisms of the dielectric constant in the paraelectric phase and the ferroelectric phase. For $T < T_0$ the value of τ is practically temperature independent, with the relaxation of ϵ' caused by the transformation (coarsening) of the domain structure. It is characteristic of the mechanism for temporal relaxation of ϵ' in the paraelectric phase in the vicinity of T_0 that the temperature dependence of τ is close to linear (fig. 12) [5].

These facts point to the complex kinetics of the ferroelectric PT in the $\text{Sn}_2\text{P}_2\text{S}_6$: the PT changes its nature

as the system approaches equilibrium. A graphic proof of this is provided by the experimental data obtained in the following circumstances. After annealing in the paraelectric phase the sample was cooled at the rate of 0.1 K min^{-1} to $T_0 + 1 \text{ K}$. As noted earlier, at this rate of temperature decrease in the paraelectric phase no departure from the Curie–Weiss law can be observed. At that temperature the sample was maintained for a certain time t (e.g., for two hours). After that the sample temperature was raised somewhat (to $T_0 + 4 \text{ K}$), and at the rate of 0.1 K min^{-1} the sample underwent a "cooling–heating" cycle in the $T_0 - 2 \text{ K}$ to $T_0 + 4 \text{ K}$ range. As the stabilization time t increases, two peaks on the ε' vs. T curve clearly manifest themselves (fig. 13). In the cooling regime the temperature distance between the peaks, $T_i - T_c$, increases with time but becomes practically constant for $t > 17$ hours (insert in fig. 13). The position of the low-temperature peak typically exhibits temperature hysteresis. The shape of the temperature anomalies in ε' remain practically unchanged when frequency varies from 10 Hz to 100 kHz . In equilibrium two peaks are also observed in the ε'' vs T dependence (fig. 14), with the low-temperature peak on the ε'' vs T lying below the respective peak on the ε' vs T curve.

The intermediate state in $\text{Sn}_2\text{P}_2\text{S}_6$ disappears after the sample is heated to a state in which it is in the paraelectric phase and also after prolonged exposure of the crystal in the ferroelectric phase. It is noteworthy that illuminating the sample with the temperature stabilized in the paraelectric phase near T_0 facilitates the formation of an intermediate state. For instance, keeping the sample in the dark at $T_0 + 1 \text{ K}$ for six hours causes two peaks to appear on the ε' vs. T curve, with the temperature interval $T_i - T_c$ between the peaks of 1.5 K , illuminating the sample with 2 mW power white light for the same time increases the interval to $T_i - T_c = 2.3 \text{ K}$.

A constant electric field applied parallel to the [100] polar axis narrows the interval $T_i - T_c$ in which the intermediate state exists. Here T_c grows linearly ($T_c(E) = T_c(0) + kE$) and T_i decreases quadratically ($T_i(E) = T_i(0) - fE^2$) as the electric field gets stronger. The intermediate state obtained by keeping the sample in the dark at $T_0 + 1 \text{ K}$ for six hours vanishes in the fields $E > 450 \text{ V cm}^{-1}$ [5]. The data prompt the conclusion that the ferroelectric second-order PT with $T_0 = 335.2 \text{ K}$ observed when the temperature varies at the rate $dT/dt > 0.1 \text{ K min}^{-1}$, commonly used in experiments, is transformed into a sequence of two transitions when the cooling rate is changed or the temperature in the critical region is stabilized: a second-order transition (T_i) and a first-order transition (T_c). The general shape of the $\varepsilon'(T)$ dependence and the presence of temperature hysteresis in the vicinity of T_c resemble the observed behaviour of the dielectric constant in the consecutive phase transitions, from the paraelectric phase to the IC phase (T_i) and from the IC phase to the ferroelectric phase (T_c), in the $\text{Sn}_2\text{P}_2(\text{Se}_x\text{S}_{1-x})_6$ crystals with selenium content $x > x_{LP} = 0.28$ [4]. The shape of the field E vs T diagrams for the intermediate state also coincides with the shape of such diagrams for the IC phases in proper fer-

roelectrics [9]. These facts suggest that the intermediate state that appears when the temperature of the $\text{Sn}_2\text{P}_2\text{S}_6$ crystal is stabilized near T_0 is an IC phase.

IV. THE PHENOMENOLOGICAL ANALYSIS OF THE RELAXATION PHENOMENON IN $\text{Sn}_2\text{P}_2\text{S}_6$ AND $\text{Sn}_2\text{P}_2\text{Se}_6$ CRYSTALS

Crystals of the $\text{Sn}_2\text{P}_2\text{S}_6$ family are ferroelectric semiconductors. The relation between the PT order parameter (spontaneous polarisation) and the charge carriers plays an important role in such crystals. This is confirmed by the strong influence of light on the memory effect in the IC phase of the $\text{Sn}_2\text{P}_2\text{Se}_6$ crystal, with a characteristic writing time of about few hours. A possible reason for the prolonged kinetics of the $\text{Sn}_2\text{P}_2\text{S}_6$ ferroelectrics in the critical region may be the relaxation of the electronic subsystem with an exponential temporal variation of the charge carrier concentration m on the trapping level in the forbidden band at fixed temperature

$$m = m_0 + \Gamma(1 - \exp(-t/\tau)). \quad (4.1)$$

For uniaxial ferroelectrics the thermodynamic potential density is given by the following series:

$$\Phi = \Phi_0 + \frac{\alpha}{2}\eta^2 + \frac{\beta}{2}\eta^4 + \frac{\delta}{2}\left(\frac{\partial\eta}{\partial Z}\right)^2 + \frac{g}{2}\left(\frac{\partial^2\eta}{\partial Z^2}\right)^2 + \dots, \quad (4.2)$$

where $\alpha = \alpha_T(T - T_0)$. The second order PT in $\text{Sn}_2\text{P}_2\text{S}_6$ is described by a potential specified by (4.2) with the following coefficients: $\alpha_T = 1.6 \cdot 10^6 \text{ Jm} \cdot \text{C}^{-2}\text{K}^{-1}$; $\beta = 7.4 \cdot 10^8 \text{ J} \cdot \text{m}^5 \text{C}^{-4}$; $\delta = 1.4 \cdot 10^{-10} \text{ J} \cdot \text{m}^3 \text{C}^{-2}$, and $g = 2.2 \cdot 10^{-27} \text{ J} \cdot \text{m}^5 \text{C}^{-2}$ [10].

For $\text{Sn}_2\text{P}_2(\text{Se}_x\text{S}_{1-x})_6$ we have $\delta \sim (x_{LP} - x)$, $\beta \sim (x_{TCP} - x)$, and $g > 0$. For $\delta < 0$ the IC phase appears with the temperature width

$$T_i - T_c \approx \frac{\delta^2}{4g\alpha_T}. \quad (4.3)$$

Following [11] we assume that α_T and δ are linear functions of m , i.e.,

$$\alpha_T(m) = \alpha_T + am, \delta(m) = \delta + bm. \quad (4.4)$$

(4.1) and (4.3) yield

$$T_i - T_c \approx \frac{[\delta + bm_0 + b\Gamma(1 - \exp(-\frac{t}{\tau}))]^2}{4g[\alpha_T + am_0 + a\Gamma(1 - \exp(-\frac{t}{\tau}))]}. \quad (4.5)$$

Thus, for $b < 0$ the $\text{Sn}_2\text{P}_2\text{S}_6$ crystal acquires an IC phase, and the phase grows with time. In the experiment

the sample was cooled from the annealing temperature $T_0 + 40$ K to $T_0 + 1$ K at a rate of $0.1 \text{ K}\cdot\text{min}^{-1}$. Under such temperature variations the electronic subsystem of the crystal remains “overheated” and at $T_0 + 1$ K tends to equilibrium as the stabilization time grows. Fig. 13 shows that the temperature interval between the two anomalies in the temperature dependence of ε' for $\text{Sn}_2\text{P}_2\text{S}_6$ does increase with time.

We estimate how a non equilibrium electronic subsystem affects the kinetics of the phase transition in the ferroelectric semiconductor $\text{Sn}_2\text{P}_2\text{S}_6$. The relaxation time τ_m of the electron concentration in the attachment levels is given by the following relation:

$$\tau_m = \{\gamma[n_0 + N_c \cdot \exp(-U_0/kT)]\}, \quad (4.6)$$

and the equilibrium concentration of such electrons is

$$m_0 = \frac{n_0 M}{n_0 + N_c \cdot \exp(-U_0/kT)}. \quad (4.7)$$

According to [3], we can assume that $\text{Sn}_2\text{P}_2\text{S}_6$ is characterized by the following parameters: $n_0 \approx 10^8$ – 10^{10} cm^{-3} , the conduction electron concentration; $N_c \approx 10^{19} \text{ cm}^{-3}$, the density of states in the conduction band; $M \approx 10^{18} \text{ cm}^{-3}$, the attachment level concentration; $U_0 \approx 0.7 \text{ eV}$, the distance on the energy scale from the bottom of the conduction band to the attachment levels; and $\gamma \approx 10^{-13} \text{ cm}^3 \cdot \text{s}^{-1}$, a rate coefficient. For $T = 335 \text{ K}$ we have $\tau_m = 5$ – 300 min and $m_0 \approx 5 \times 10^{14} \text{ cm}^{-3}$ [5].

The coefficient a in (4.4) is determined by the electron-phonon interaction and its value can be found from the data on the variation, induced by spontaneous polarization, of the band gap in the ferroelectric phase: $Eg = Eg_0 + a\eta^2$. According to the data of [5], $a = 10^{-18} \text{ J}\cdot\text{m}\cdot\text{C}^{-1}$ for $\text{Sn}_2\text{P}_2\text{S}_6$.

The insert in fig. 13 shows the time dependence, calculated by (4.5), of the temperature interval $T_i - T_c$ for the intermediate state, which emerges if the $\text{Sn}_2\text{P}_2\text{S}_6$ crystal is kept in the critical region for a long time.

Charge carriers play a dominant role in the memory effect in the crystal studied. Indeed, spatial modulation of impurity level energy which is determined by a spontaneous polarization square distribution results in the modulation of excitation probability for charge carriers and, hence, in incommensurate distribution of carriers over the traps. The results [7] from the thermally stimulated current strongly favour the idea of an electronic nature of the memory effect in $\text{Sn}_2\text{P}_2\text{Se}_6$. The peak of temperature dependence of the current at approximately 230 K corresponds to the temperature, heating above which leads to an abrupt suppression of the memory effect anomaly (fig. 10). Moreover the thermally stimulated current disappears completely at around 240 K, which coincides with the temperature heating above which the anomaly vanishes.

The theory of the memory effect caused by these trapped charge carriers has been elaborated in [3]. The

principle of this model is based on the appearance of an inhomogeneous density of carriers on the trap levels due to the modulation of the energy of the local centre in the band gap. The density of electrons at the trap levels is defined by a homogeneous m_0 and an inhomogeneous components: $m = m_0 + m_l(z)$. The inhomogeneous density is described by

$$m_l \approx \frac{N_c \cdot \exp(-U_0/kT) \tilde{a} m_0 / kT}{n_0 + N_c \cdot \exp(-U_0/kT)} P_q^2, \quad (4.8)$$

where \tilde{a} is the coefficient in the expression $U = U_0 + \tilde{a} P_q^2$, which describes the dependence of the interval between the bottom of the conduction band and trap levels on the order parameter P_q .

We will assume the coupling potential between the modulation order parameter (P_q) and the electronic induced polarisation (P_{in}) to be linear. Let us present P_{in} in the form $P_{in} = m_l(z) P_0$, where $m_l(z)$ is the density of the electrons trapped by the local centres given by (4.8) and P_0 is the effective dipole moment of the recharged centres. Following [2] the coupling potential can be written as

$$V = V_0 m(z) P_0 P_q \delta(qq^*), \quad (4.9)$$

where $q^* = q(T^*)$ corresponds to the wave number of the sinusoidal modulation of the induced electronic polarization. The temperature interval within which the wave number q^* is locked is given by [2]

$$\Delta T = \frac{\sqrt{2}}{\pi} \cdot \frac{(V P_q^{-2})^{1/2}}{\delta^{1/2} \varsigma}, \quad (4.10)$$

where $\varsigma = (dq/dT)|_{q=q^*}$ and δ is the coefficient in (4.2). Inserting the expressions for the coupling potential (Equation (4.9)) and the density of charge carriers on the trap level (Equation (4.8)) into Equation (4.10) ΔT is expressed by

$$\Delta T = \frac{\sqrt{2}}{\pi \delta^{1/2} \varsigma} \times \frac{(V_0 N_c \exp(-U_0/kT) \tilde{a} m_0 P_q / kT)^{1/2}}{n_0 + N_c \exp(-U_0/kT)}. \quad (4.11)$$

In this formula the time dependence of the density of the recharged centres has not been taken into account. It is assumed that $P_q \sim (T_i - T)^{1/2}$. A fit of (4.11) to the experimental temperature dependence of ΔT (fig. 10) gives $U_0 = 0.42 \pm 0.01 \text{ eV}$, $N_c = 10^{19} \text{ cm}^{-3}$ and $n_0 \sim 9 \cdot 10^9 \text{ cm}^{-3}$ as parameters [7].

As can be seen from fig. 10, b, ΔT tends to saturation with an increase in the temperature stabilization time interval. The solid line in fig. 10, b is a fit to an exponential variation of $\Delta T = 0.49 + 0.79(1 - \exp(-t/\tau))$ with $\tau \sim 100 \text{ min}$. According to model [3], in which the mem-

ory effect is related to the inhomogeneous distribution of charge carriers on the trap levels the time τ constant can be attributed to the charge carrier relaxation on the trap levels. This time relaxation is determined by Equation (4.6).

Using for $\text{Sn}_2\text{P}_2\text{Se}_6$ $n_0 \sim 9 \cdot 10^9 \text{ cm}^{-3}$, $N_c = 10^{19} \text{ cm}^{-3}$ and $U_0 = 0.4 \text{ eV}$, $T = 196 \text{ K}$ and $\gamma \approx 10^{-13} \text{ cm}^3 \cdot \text{s}^{-1}$ (typical for wide-band-gap semiconductors [3]), τ is found to be equal to about 140 min. This value is in reasonably good agreement with that obtained from the dependence of ΔT on writing time.

It should be noted that, in the case of a defect mechanism of the memory effect, the defect concentration providing the pinning of the incommensurate modulation with a wavelength of 12–15 elementary cells should be very large: of the order of 10^{20} – 10^{21} cm^{-3} . Such concentrations are only tolerable for "proper defects" of the crystal lattice. The recharging of the ions may be one of the mechanisms in creating this kind of defects. In the case of the $\text{Sn}_2\text{P}_2\text{Se}_6$ crystals one can assume the following mechanism. Through the electron–phonon coupling the free charge carriers are localised near the $(\text{P}_2\text{Se}_6)^{4-}$ anion quasimolecular groups, creating quasiparticles similar to the polaron. However, this is only one of the possible configurations which can be generated in the crystal by the recharging effect.

V. CONCLUSIONS

The observation of the thermal memory effect for the IC-phase $\text{Sn}_2\text{P}_2\text{Se}_6$ ferroelectric–semiconductor allowed to establish the following regularities. The manifestation of the effect in the low-frequency dielectric properties and optical birefringence is similar. The state of the electron subsystem of $\text{Sn}_2\text{P}_2\text{Se}_6$ crystals determines conditions for the memory effect recording: the effect has been observed in the low-resistant samples and it was not noticed for the high-resistant ones, the effectiveness of recording depending on the light wave-length. Thermal memory in the IC-phase of $\text{Sn}_2\text{P}_2\text{Se}_6$ within described in the framework of the phenomenological model assuming spatial

redistribution in the wave-field of spontaneous polarization of the charge carriers concentration on the impurity energy level in the forbidden band of the crystal.

The observed long term relaxation of the dielectric parameters in the paraelectric phase of the $\text{Sn}_2\text{P}_2\text{Se}_6$ crystals and the appearance of a state intermediate between the paraelectric and ferroelectric phases (apparently, an IC phase) is also described within the framework of the phenomenological model, assuming renormalization of the thermodynamic potential constant with a variation in the concentration of charge carriers on the impurity energy level in the forbidden band. It should be noticed that the thermal memory effect in the IC phase of $\text{Sn}_2\text{P}_2\text{Se}_6$ and the relaxational appearance of the intermediate state in $\text{Sn}_2\text{P}_2\text{Se}_6$ are agreeably described with account of the previously determined data of the thermodynamic potential constants for these crystals and the adequate values of the semiconductor parameters.

Thus, using $\text{Sn}_2\text{P}_2\text{S}_6$ and $\text{Sn}_2\text{P}_2\text{Se}_6$ proper ferroelectrics with semiconducting properties as examples, we have investigated and compared two types of relaxation phenomena caused by a interrelation between the phase transition order parameter and mobile defects–charge carriers. The renormalization of spatial dispersion of the stiffness coefficient for the order parameter fluctuations, caused by the change in the charge carriers concentration on the impurity energy level, shifts the position of the Lifshitz point on the state diagram and leads to the IC phase appearance in the $\text{Sn}_2\text{P}_2\text{S}_6$ crystal. At the same time the local centres energy modulation in the forbidden band of the $\text{Sn}_2\text{P}_2\text{Se}_6$ semiconductor, caused by the non-uniform static field of the order parameter in the IC phase, leads to the appearance of the charge carriers concentration wave, which is displayed through the thermal memory effect.

VI. ACKNOWLEDGMENTS

The authors wish to thank A.P.Levanyuk for helpful discussions. This work has been supported by the Project INTAS–93–3230.

-
- [1] J. P. Jamet, P. Lederer, *J. Phys. Lett. (Paris)* **44**, L257 (1983).
 - [2] P. Lederer, G. Montambaux, J. P. Jamet, M. Chauvin, *J. Phys. Lett. (Paris)* **45**, 627 (1984).
 - [3] R. F. Mamin, *Sov. Phys. Solid State* **33**, 1473 (1991).
 - [4] Yu. M. Vysochanskii, V. Yu. Slivka, *Sov. Phys. Usp.* **32**, 123 (1992).
 - [5] A. A. Molnar, Yu. M. Vysochanskii, A. A. Horvat, Yu. S. Nakonechnii, *Zh. Eksp. Teor. Fiz.* **79**, 945 (1994).
 - [6] Yu. M. Vysochanskii, M. M. Major, Sh. B. Molnar, S. F. Motrja, S. I. Perechinskii, V. M. Rizak, *Sov. Phys. Crystallogr.* **36**, 699 (1991).
 - [7] M. M. Major, Th. Rasing, S. W. Eijt, P. H. van Loosdrecht, H. van Kempen, S. B. Molnar, Yu. M. Vysochanskii, S. F. Motrja, V. Yu. Slivka, *J. Phys.: Cond. Matt.* **6**, 11211 (1994).
 - [8] Yu. M. Vysochanskii, A. A. Molnar, A. A. Horvat, Yu. S. Nakonechnii, *Ferroelectrics* **169**, 141 (1995).
 - [9] D. Durand, F. Denoier, D. Lefur, *J. Phys. Lett.* **44**, 207 (1983).
 - [10] Yu. M. Vysochanskii, M. M. Major, V. M. Rizak, V. Yu. Slivka, M. M. Khoma, *Sov. Phys. JETP* **68**, 782 (1989).
 - [11] R. F. Mamin, *Crystallogr. Rep.* **38**, 74 (1993).

**РЕЛАКСАЦІЙНІ ЯВИЩА В КРИСТАЛАХ ВЛАСНИХ ОДНОВІСНИХ
СЕГНЕТОЕЛЕКТРИКІВ–НАПІВПРОВІДНИКІВ $\text{Sn}_2\text{P}_2\text{S}(\text{Se})_6$
З НЕСПІВВИМІРНОЮ ФАЗОЮ**

Ю. Височанський, А. Молнар

*Ужгородський державний університет, Інститут фізики і хімії твердого тіла
Україна, UA-294000, Ужгород, вул. Підгірна, 46*

Для кристалів сегнетоелектриків–напівпровідників $\text{Sn}_2\text{P}_2\text{S}(\text{Se})_6$ релаксація електронної підсистеми зумовлює зсув точки Ліфшиця на фазовій діаграмі і пінінг хвилі параметра порядку “ефект пам’яті” в неспіввимірній фазі. Для цих власних одновісних сегнетоелектриків обидва ефекти задовільно описуються феноменологічною моделлю, яка припускає: перенормування просторової дисперсії коефіцієнта жорсткості для флюктуацій параметра впорядкування внаслідок релаксаційної зміни концентрації носіїв заряду на домішковому енергетичному рівні в забороненій зоні кристалу; зумовлену неоднорідним статичним полем параметра порядку в неспіввимірній фазі модуляцію енергії локальних центрів, яка веде до появи концентраційної хвилі носіїв заряду.